Original Research

Serum levels of immunoglobulin and complement in UTI of patients caused by *Proteus mirabilis* and using AgNPs as antiswarming

Kamal Ismael Bakr Al Otraqchi[1], Suhaila Nafee Darogha[2*], Beriwan Abdulqadir Ali[3,4]

[1] Lecturer at Basic Science Department, College of Medicine, Hawler Medical University, Erbil, Kurdistan Region-Iraq

[2] Department of Biology, College of Education, Salahaddin University-Erbil, Erbil, Kurdistan Region- Iraq

[3] Department of Physiotherapy, Erbil Technical Health College, Erbil Polytechnic University, Erbil, Kurdistan Region- Iraq

[4] Department of Pharmaceutical Basic Sciences, Faculty of Pharmacy, Tishk International University, Erbil, Kurdistan Region- Iraq

Abstract: The use of plant extracts represents a promising approach for the synthesis of silver nanoparticles (AgNPs). This study reports the low-cost, green synthesis of AgNPs using the extract of clove and black seeds. The biosynthesized AgNPs were confirmed and characterized by analysis of the spectroscopy profile of the UV-visible spectrophotometer. The purpose of the present study is to evaluate the inhibitory effect concentration (MIC) of AgNPs, clove, and black cumin seed extracts on the growth and swarming of *P. mirabilis*. Clinical isolates of *P. mirabilis* were isolated from patients suffering from urinary tract infections. Thirteen types of antibiotics were used in the present study to detect their ability to inhibit *P. mirabilis*'s resistance. Immunological findings included the determination of serum levels of IgG, IgM, IgA and complement protein C3 and C4. Results showed that IgG and IgA concentrations significantly increased (1311.13 ± 72.54 and 279 ± 21.31) respectively in UTI patients in comparison to the healthy control group which was 1089.88 ± 37.33 and 117.611 ± 4.19 respectively, While IgM concentrations were increased non significantly in UTI patients (153.331 ± 6.45) in comparison to healthy control (145.2 ± 13.49). Complement components C3 showed a significant increase in UTI patients with mean values of 125.95 ± 6.22 compared to the control group with mean values of 55.191 ± 9.64, while C4 showed statically non-significant among UTI patients in comparison with the control group (35.195 ± 2.34 and 34.371 ± 1.22) respectively.

Key words: UTI; Immunoglobulin; Complement; *Proteus mirabilis*; Swarming; AgNPs; Clove; Black cumin seeds.

Introduction

Urinary tract infections (UTI) are mostly of the ascending type, hence, urinary tract mucosa including urinary immunoglobins (secretory IgA) is considered as the frontline of defense against bacterial infection. Local immunoglobulin of the urinary tract serves as defending agents that inhibit bacterial attachment to mucosal surfaces (1). Serum antibodies found in UTI-positive patients have bactericidal activity (2). Antibodies in urine may resist UTI by preventing the adherence of bacteria to uroepithelial cells, the role of humoral immune response which increased IgG and IgA, IgM production were associated with UTI. Also, bacteria are killed by infected human serum through the lytic activity of the complement system. Complement 3 (C3) levels are significantly higher in the urine of UTI patients and uropathogenic *E. coli* may stimulate C3 production (3). UTIs are one of the human infectious diseases caused by a bacterial infection that affects any part of the urinary tract (4). UTIrepresents one of the most common types of infections in the human body. Various bacteria are involved in the development of UTI, including *Escherichia coli, Klebsiella, Pseudomonas, Proteus mirabilis* and *Enterococcus faecalis*. It is the second most frequent kind of infection in the body. Bacterial organisms which cause UTI may involve *Escherichia coli, Klebsiella, Pseudomonas, Proteus mirabilis* and *Enterococcus faecalis*. less than 8% of uncomplicated UTIs is caused by *Proteus mirabilis*, a major pathogen often isolated from patients with complicated UTIs, i.e., those with functional or anatomic abnormalities of or with chronic foreign bodies in the urinary tract (5). As a motile gram-negative bacillus belonging to the family Enterobacteriaceae, *P. mirabilis* represents an opportunistic pathogen frequently found in intestinal tracts (6). *P. mirabilis* is considered a major cause of UTIs and the primary infectious factor in patients with indwelling urinary catheters (7).

P. mirabilis can cause food poisoning, respiratory and wound infections, bacteremia, and other infections. *P. mirabilis* infection is due to the presence of a wide range of virulence factors, including the presence of extracellular proteins, motility of the pathogen by flagella, the activity of urease enzymes, binding to iron ions, invasion of cells, and so on. Lipopolysaccharides and hemolysins are also two important virulence factors that allow bacteria to attach to cells and colonize tissues, thus exacerbating pathogenesis. It should be noted, however, that the pathogenicity of this bacterium is not solely due to virulence genes; biofilm formation is also one of the main factors in the pathogenicity of *P. mirabilis*, which plays an important role in the persistence of infection and the occurrence of inflammatory reactions

(6). After bacterial colonization, the catheter may enter the bladder, setting the stage for UTI(8).

Swarming and migration improve the ability of *P. mirabilis* to colonize the catheter and urinary tract. Swarming refers to the transformation of small, motile vegetative cells into multinucleated and aseptate swarms that are up to forty times larger than vegetative cells and have much larger flagella. These swarms migrate rapidly from the colony until they are paused (consolidated) and begin de-differentiation. The sequence of migration and consolidation cycles leads to the formation of larger colonies, which is characterized by the presence of concentric rings (9). It should be noted that biofilm formation plays a critical role in this migration (10). The transformation of vegetative cells into large, multinucleated and hyperflagellated swarms is one of the most important reasons for the retention of *P. mirabilis* pathogenicity. This is a banishment of the bacterial response to growth in viscous fluids. Swarm requires a lot of resources; in a way, a large part of the bacterial metabolism is allocated to the assembly and operation of the flagellum and other proteins involved in the swarm. This differentiation is due to the coordinated expression of the global regulon of 50 genes. These proteins contain a large set of virulence factors including flagellin, urease, hemolysin, and the ZapA metalloprotease degrading antibacterial peptides, such as defensin one and LL-37. Due to the coordinated expression of virulence factors during differentiation, it is believed that the transformation of vegetative cells into swarmer cells plays a key role in pathogenicity (11).

Nanoparticles represent a particle with a nanometer size of 1–100 nm. The nanoscale material has new, unique, and superior physical and chemical properties compared to its bulk structure due to an increase in the surface area's ratio per volume of the material/particle (12). Silver nanoparticles have found many applications in the medical industry due to their antibacterial properties and inhibitory effects on microbial growth (13). Due to the importance of silver nanoparticles, various methods such as chemical reduction, photochemical reduction, integrated methods, micro-emulsion radiation and green synthesis have been proposed to produce these particles (14). Recently, the use of herbal extracts has sometimes been proposed as a fast, cost-effective and environmentally friendly approach to the production of metal nanoparticles. By using such a green method, the toxicity of nanoparticles can be reduced and the problems related to chemical methods such as high cost and environmental pollution can be avoided. So far, many studies have shown that silver nanoparticles produced using plant extracts have antimicrobial and anticancer properties (15).

Swarming cell formation is an important feature of *P. mirabilis* infection. Swarming refers to the formation of bacterial concentric zones that cover the entire surface of the culture medium (8). Due to the occurrence of swarming, it is very difficult to isolate other bacteria from cultures containing *P. mirabilis*. At the same time, it should be borne in mind that swarming is a major problem for laboratory diagnostic activities. Therefore, the development of methods that can prevent the formation of swarms without harming other bacteria is clinically important. It is through swarming that bacteria can

spread in the form of biofilms throughout the culture medium (16). This study is aimed to evaluate the effect of AgNPs of clove and black seed cumin on the swarming of *P. mirabilis*.

Materials and Methods

Sample collection and identification

Ethical approval for this research was confirmed by the scientific and ethics committee of Salahaddin University-Erbil of Iraq. A total of 283 samples from patients with UTI symptoms were screened, and finally, 51 isolates (18.02%) of P. mirabilis were isolated. The specimens were directly inoculated to Tryptone Soy Broth and streaked onto MacConkey agar and Blood agar plates and incubated aerobically at 37 °C for 24 hrs. The isolates were identified based on a series of microbiological and biochemical tests that routinely are used in microbiological diagnostic laboratories and confirmatory VITEK II system using (ID) GN cards (BioMérieux Inc. France). All positive cultures were undergoing the PCR assay for amplifying the ID gene to support the identification of *P. mirabilis*.

Molecular characterization of the isolates

For more confirmation of the identity of isolates, all *P. mirabilis* isolates were subjected to molecular characterization by detecting a specific gene or responsible to produce urease enzyme and regarded as a diagnostic feature of these bacteria using PCR.

Genomic DNA extraction

The confirmed DNA was used to amplify the *ureR* gene in P. mirabilis isolates. The sequence of the *ureR* gene was used to confirm the identity of *P. mirabilis*; short read sequence products of 225 bp length as amplicon size were produced with Z18752F 5′-ATA ATC TGG AAG ATG ACG AG-3' and Z18752R 5′-GGT GAG ATT TGT ATT AAT GG-3' (17). Briefly, PCR reaction of these genes was carried out in a total volume of 25 μL with the program: an initial denaturation at 94 °C for 4 mins, followed by 40 cycles, each consisting of denaturation at 94 °C for 40 sec; annealing at 58 °C for 1 min; extension at 72 °C for 20 sec, and a final extension at 72 °C for 10 mins. Then, the amplified samples were electrophoresed on agarose gel containing ethidium bromide to observe the PCR products.

Antibiotic susceptibility testing

The P. mirabilis isolates were subjected to antibiotic susceptibility testing against thirteen antibiotics by disk diffusion. The antibiotics tested against the isolates were including amikacin (30μg), ceftazidime (30μg), cefepime (30 μg), gentamicin (10 μg), aztreonam (30 μg), piperacillin (10 μg), imipenem (10 μg), meropenem (10 μg), tobramycin (10 μg), levofloxacin (10μg), ciprofloxacin (5 μg), tetracycline (30 μg), and netilmicin (10 μg). The inhibition zone diameter (mm) of each antimicrobial disc was measured.

Extraction of clove and black seed

A 10 g weight of powdered clove (18) and black cumin seeds (19) was suspended in 100 mL of sterilizing distilled water and shaken at a constant rotating speed of

150 rpm/min in a shaker for 48 hrs. It was centrifuged for 10 min at 4000 ×*g* and filtered through filter paper to get a clear extract. A concentration of 10.0 mg. mL^{-1} stock solution was prepared using distilled water via the serial dilution method.

Biosynthesis of silver nanoparticles

The synthesis of silver nanoparticles was achieved by dissolving AgNO$_3$ powder in distilled water to prepare a 10 mM *stock solution* (20). Mix extract with AgNO$_3$ (1:10 ratio) in the flask 250 mL and wrapped with an aluminum foil and was then heated in a water bath at ~2 hrs. at 90 ºC. The reaction mixture was adjusted to pH 10.0 by adding 1.0 M NaOH solution drop-by-drop to allow the magnetic precipitations to form uniformly. The reduction process of silver ions (Ag$^+$) to silver (Ag^0) nanoparticles was identified by the color change of solutions from yellow to brownish-yellow or deep brown depending on the reaction condition (21). After that, the AgNPs were obtained by repeated centrifugation at 10 000 ×*g* for 20 min, and then, discarded the supernatant and the pellet was washed using deionized water several times. The obtained samples were dried overnight in a vacuum oven at 60 °C and collected (20).

Characterization

UV–Visible absorption analysis was carried out by using a Shimadzu single-beam UV–Visible spectrophotometer in the range of 200–800 nm to study the successful formation of AgNPs. FT-IR spectroscopy analysis was carried out by using a Shimadzu 100 FTIR spectrometer in the range of 400–4000 cm^{-1} by crushing a small amount of sample AgNPs and plant extract with KBr powder to study the functional groups (22).

Ferric reducing antioxidant power (FRAP) assay

FRAP reagent was freshly prepared by the protocol of (15). Overall, 10 µL of extracts and AgNPs (0.1 mg. mL^{-1}) was distributed into a 96-well plate, and then 200 µL of FRAP reagent was placed into the same well containing the sample. The solution was mixed and incubated for 30 min at 37 °C. The absorbance was recorded at 593 nm. A dark blue color formed as the Fe^{3+}–TPTZ complex was reduced to Fe^{2+}–TPTZ form by the anti-oxidant. The standard ascorbic acid curve was prepared for comparison using various concentrations, as shown in Figure 1. The following equation calculates the FRAP value for each compound.

$$\text{FRAP value of the sample (µM)} = \text{Abs. (sample)} \times \frac{\text{FRAP value of standard (µM)}}{\text{Abs. of standard}}$$
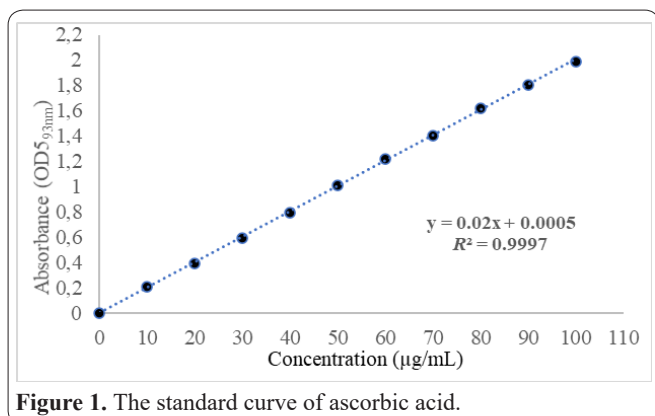
Figure 1. The standard curve of ascorbic acid.

Antibacterial activity of extracts and AgNPs

Antibacterial potential analysis by agar disk diffusion method

The cultures of *P. mirabilis* inappropriate agar plates were conducted for the disk diffusion assay. Briefly, 100 µL of bacterial suspension (~1 × 10^8 CFU. mL^{-1}), previously overnight cultivated in LB broth at 37 °C, was spread on the surface Mueller-Hinton agar plates. Then, five sterilized filter disks were placed on the agar plates conducted with 40 µL of the appropriate concentration of extracts and AgNPs at 45-50 °C. The plates were incubated at 37 °C (24 hrs.), and the relative clear zones of microbial inhibition were estimated in millimeters (mm). The antimicrobial activity of the extracts and AgNPs was determined from the clear zones of inhibition. For this purpose, the concentrations 512, 256, 128, 64, and 32 µg. mL^{-1} of the extracts and AgNPs were used to study disk diffusion. Gentamicin (10 µg) and DMSO (%5) were prepared as positive and negative controls, respectively (13).

The minimum inhibitory concentration (MIC)

The MIC and the minimal bactericidal concentration (MBC) of extracts and AgNPs were determined following Clinical and Laboratory Standards Institute (CLSI) guidelines. Bacteria cells were inoculated in the wells of a 96-microwell plate containing either LB broth alone (positive control) or LB broth containing AgNPs at a final concentration ranging and extracts performed the same protocol with different concentrations ranging from 32-512 µg. mL^{-1}. The microplates were incubated at 37 ºC for 24 hrs. at 250 rpm. The MIC value corresponded to the extracts and AgNPs doses that inhibited bacterial growth (compared to the positive control). MBC was also evaluated by sub-culturing the content of the first two clear wells obtained in the MIC assay onto LB agar plates (23). Amoxicillin (100 µg. mL^{-1}) was used as the control for this bacterium. Optical density at 630nm (OD$_{630}$) was used to estimating the concentration of the bacterial population via ELISA reader (24).

Tolerance level

The tolerance level of tested bacterial strains against AgNPs and extracts was determined using the following formula (25): $Tolerance = MBC/MIC$

The characteristic of the antibacterial activity of AgNPs was determined by the tolerance level indicating the bactericidal or bacteriostatic action against the *P. mirabilis*. When MBC/MIC ratio is ≥16, the test agent's antibacterial efficacy is considered bacteriostatic, whereas MBC/MIC ≤4 indicates bactericidal activity.

Inhibition of the swarming phenomenon

Swarming motility experiments were performed as described by Aygül et al., 2019 (26). LB broth with 1.5% agar containing extracts and AgNPs at the required concentration were prepared. As a positive control, boric acid was used in swarming motility experiments. The plates could dry at 37 °C for 24 hours. After that, 1 mL of a fresh overnight culture of bacteria in LB broth was taken into a sterile microcentrifuge tube, and the cells were precipitated by centrifugation (12.000 ×*g*

Kamal Ismael Bakr Al Otraqchi *et al.*

Serum levels of immunoglobulin and complement in UTI of patients.

for 1 min). The supernatant was then discarded, 1 mL of 0.9% sodium chloride solution was added, and the residual bacteria were resuspended by vertexing. Five μL suspensions were added to the center of the dried plates. The plates were incubated reversely at 37 °C for 24 hrs. After 24 hrs., the diameter of the swarm circle was measured in millimeters and recorded. In triplicate experiments, the mean of swarm diameters detected on three plates was taken, and the results were analyzed compared with the negative control group.

Assessment of biofilm production of *P. mirabilis*

The biofilm formation by *P. mirabilis* was assessed according to Stefanovic 2000 with some modifications. Fresh tryptone soya broth (TSB) was added to an overnight culture of *P. mirabilis* to adjust its turbidity to 10^6 CFU. mL^{-1}. The wells of microplates were inoculated with aliquots of 200 μL of the adjusted bacterial suspension, and the plates were incubated for 24 h at 37 °C. The wells were gently aspirated and then washed thrice with sterile phosphate-buffered saline (PBS, pH 7.2) to remove any non-adherent cells. To fix the adherent cell, 200 μL of 99% methanol were added and left for 20 min. The wells were stained with 200 μL crystal violet (1%) for 20 min, and the unbound dye was removed under running distilled water and dried in air. The bound dye was eluted by adding 160 μL of 95% ethanol, and the optical densities of the stained adherent biofilms were read with a microplate reader at a wavelength of 490 nm. The test was repeated three times, and the average optical densities were calculated. The cut-off OD (ODc) that corresponds to three times standard deviations above the mean OD of the negative control was calculated, and the biofilm formation capacity was assessed as non-biofilm forming (OD ≤ODc), weak biofilm forming (OD > ODc, but ≤ 2ODc), moderate biofilm-forming (OD>2ODc, but ≤ 4ODc), or strong biofilm-forming (OD> 4ODc) (Table 1) (27).

Assay of immunoglobulins and complements in serum

Venous blood samples (3 ml) were collected from UTI patients and control groups, sera were separated and stored at deep freeze until analysis of serum levels of immunoglobins (IgG IgA IgM) and complement (C 3, C 4) were estimated by using commercially available Immunokits of Biomerieux France, based on the principle of single radial immunodiffusion (28,29). After placing 5 ul of serum samples on each well on plates (IgG IgA IgM) as well as C 3 and C 4 the plates were incubated for 72 hours for IgG, IgA, C3 and C4 and 96 hours for IgM at room temperature. At the end of this period, the diameter of precipitation was measured and converted mg/dl units using a table supplied by the manufacturer.

Results

Isolation of *P. mirabilis*

Out of 283 clinical specimens of UTI sources, 51 isolates (18.02%) were identified as *P. mirabilis*. The percentages of *P. mirabilis* isolated from various clinical specimens are presented in Figure 2.

Identification of *P. mirabilis* isolates

The isolates were first identified as related to the genus *P. mirabilis* by swarming phenomenon on blood agar, the characteristic smell of cultures. Microscopic examination of the bacteria appeared as straight rods and gram-negative when it was stained with Gram stain. Several conventional biochemical tests were done to characterize the suspected *P. mirabilis* isolates. All the 51 isolates of *P. mirabilis* were confirmed with VITEK II compact system.

Molecular characterization of *P. mirabilis* isolates

All isolates of *P. mirabilis* underwent a PCR assay to confirm these isolates' identity, using the *ureR* gene to detect *P. mirabilis*. Results of molecular identification shown in Figure 3 indicated that all *P. mirabilis* isolates were positive for the presence of *ureR* gene at 225 bp amplicon size. Generally, all 51 isolates of *P. mirabilis* (100%) exhibited positive PCR products on gel electrophoresis for the *ureR* gene at 225 bp.

Antibiotic susceptibility patterns of *P. mirabilis* isolates

The susceptibility patterns of the *P. mirabilis* isolates
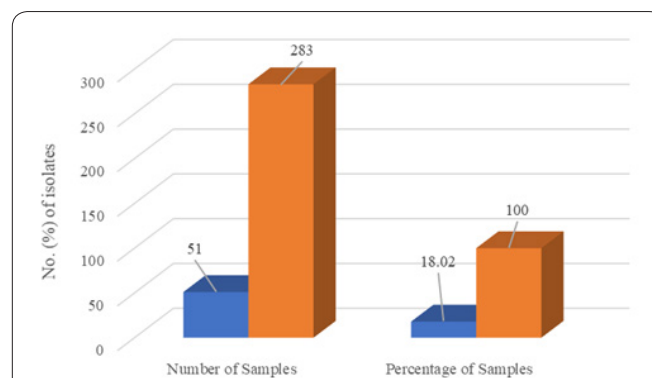
Figure 2. Number (%) of *P. mirabilis* isolated from UTI clinical specimens.
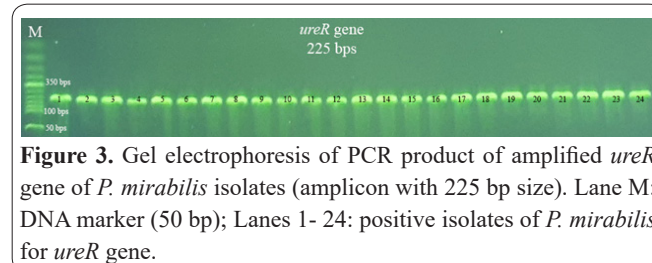
Figure 3. Gel electrophoresis of PCR product of amplified *ureR* gene of *P. mirabilis* isolates (amplicon with 225 bp size). Lane M: DNA marker (50 bp); Lanes 1- 24: positive isolates of *P. mirabilis* for *ureR* gene.

Table 1. Classification of biofilm formation abilities by Microtiter plate method.

Cut-off value calculation	Mean of OD$_{570}$ values results	Biofilm formation abilities
ODnc > 4ODc	OD > 0.557	Strong
2ODc < ODnc ≤4ODc	0.278< OD ≤ 0.557	Moderate
ODc< ODnc ≤ 2ODc	0.139< OD ≤ 0.278	Weak
OD ≤ 0.139	OD ≤ 0.139	None

Table 2. Antibiotic susceptibility patterns of *P. mirabilis* isolates toward thirteen antimicrobials.

Antimicrobials	Disk potency (μg)	Antimicrobial's symbol	Number of *P. mirabilis* (*n*=211) isolates with susceptibility			Resistant percent of *P. mirabilis* isolates
			S	I	R	
Amikacin	30	AK	48	0	3	6.16
Aztreonam	30	AZT	0	0	51	100.00
Cefepime	30	CEF	3	1	47	91.47
Ceftazidime	30	CET	0	6	45	87.68
Ciprofloxacin	5	CIP	3	1	47	91.47
Gentamicin	10	G	12	38	1	2.37
Imipenem	10	IM	4	0	47	91.47
Levofloxacin	10	LEV	14	1	36	70.14
Meropenem	10	MER	51	0	0	0.00
Netilmicin	10	NET	25	0	26	51.18
Piperacillin	10	PIP	0	3	48	93.84
Tetracycline	30	T	0	0	51	100.00
Tobramycin	10	TOB	21	0	30	59.72

*n: Number of isolates, S: Sensitive, I: Intermediate, R: Resistant. AK: amikacin; AZT: aztreonam; CEF: cefepime; CET: ceftazidime; CIP: ciprofloxacin; G: gentamicin; IM: imipenem; LEV: levofloxacin; MER: Meropenem; NET: netilmicin; PIP: piperacillin; T: tetracycline; TOB: tobramycin.

are presented in Table 2. It was found that the more effective antibiotic against isolates was the Meropenem, where all isolates of *P. mirabilis* were sensitive to it. Adversely, the less effective antibiotic was tetracycline when all isolates resisted them. However, the effect of other antibiotics was variable among the *P. mirabilis* isolates.

Antibiotic resistance profile revealed that a vast resistance was generally detected among the *P. mirabilis* isolates against the antibiotics used. It was found that out of 51 isolates of *P. mirabilis* isolates, 100% resistance property was found to aztreonam and tetracycline, more than 90% resistance to cefepime, ciprofloxacin, imipenem, and piperacillin; and about 70% or less resistance pattern was identified to amikacin, gentamicin, levofloxacin, netilmicin, and tobramycin. Variable degrees of resistance by (6) was recorded of 176 isolates of *P. mirabilis* to all antibiotics tested were observed. The resistance to doxycycline was the highest (112, 63.64%), followed by ampicillin (104, 59.09%), ciprofloxacin (101, 57.39%), streptomycin (98, 55.68%), tetracycline (97, 55.12%), piperacillin/tazobactam (88, 50%), cefotaxime (86, 48.87%), sulfamethoxazole (76, 43.19%), nitrofurantoin (75, 42.61%), polymyxin B (69, 39.2%), ceftriaxone (67, 38.07%), kanamycin (67, 38.07%), ceftazidime (62, 35.23%), gentamicin (60, 34.09%), cephalothin (53, 30.12%), cefoperazone (50, 28.41%), levofloxacin (45, 25.57%), meropenem (44, 25%), and imipenem (36, 20.45%). Of the sensitive strains, meropenem (57.96%) and imipenem (64.78%) showed the strongest antimicrobial effect on *P. mirabilis*.

Reducing the power of AgNPs and extracts

Reducing power assay is a new approach used to analyze various medicinal plants to detect anti-oxidant activities and reduce Fe^{3+} to Fe^{2+}. This is because anti-oxidants are potent agents of reduction. Many researchers have also documented that the decrease of bioactive compounds is linked to antioxidant activity (30). The anti-oxidant activity of the clove, black cumin seeds,

Table 3. Anti-oxidant activity of the AgNPs and extracts measured by FRAP assay.

Extract and compounds	Absorbance	FRAP value (μM)
Clove	2.78	155.7142
AgNP-Clove	2.98	166.9166
Black cumin seed	2.69	150.6731
AgNP-Black cumin seed	2.41	134.9896
Ascorbic acid	2.194	122.891

and ascorbic acid was measured by FRAP assay. Extracts and AgNPs of both clove and black cumin seeds indicate that they are the most effective electron donor and can reduce the oxidized intermediates highly reactive molecules like free radicals and reactive oxygen species of peroxidation processes and the FRAP value was 155.7142 μM, 150.6731 μM for clove and black cumin seeds extract when compared with ascorbic acid. Ascorbic acid is usually used as a standard for preparing the standard curve and has high antioxidant activity (FRAP value = 122.891 μM). Hence, it is essential to determine the reducing power of phenolic constituents to explain the relationship between their anti-oxidant effects (Table 3).

UV-Visible spectra of AgNPs

The UV-Vis spectra were captured of AgNPs with extracts, where distilled water was used as a blank. As illustrated in Figure 4, the absorbance peak was observed at 450 nm. Increased intensity is due to the excitation of surface plasmon resonance (SPR) in the AgNPs, implying the formation of silver nanoparticles. Because the synthesis environment, as well as the shape and size of the nanoparticles, affect the rate of SPR adsorption, as the concentration of nanoparticles increases, the plasmon bands expand and show an absorption tail. This phenomenon indicates an increase in the size distribution of nanoparticles. Previous studies have reported the effect of silver nanoparticles on the formation of

adsorption bands at 400 nm. The SPR band for silver nanoparticles has also been reported at around 435 nm (31) (Figure 4).

(32) reported that the color change of the synthesis mixture (herbal extract and silver nitrate as substrate) represents the formation of silver nanoparticles. This agrees with the results of (33) who remarked the color change as an indicator of nanoparticle formation. Surface-active particles have been proposed by (34) as crucial agents in the formation of silver nanoparticles. As a result of electrostatic interactions, functional agents contained in herbal extract interact with silver ions and transform them into nanoparticles. Some of the functional agents in herbal extract involved in the formation of nanoparticles include Flavones, amides, carboxylic acid, aldehydes, ketones, terpenoids, quinines, and anthraquinones (35).

Fourier transform infrared spectroscopy analysis

FTIR analysis was carried out for the identification of possible biomolecules present in the plant extract responsible for the reduction of Ag^+ into Ag^o. FTIR spectra of AgNPs and plant extracts are present in Figure 5. The spectrum of AgNP-Black seed shows different main peak positioned at 1406 cm^{-1}, 1467 cm^{-1}, 1517 cm^{-1}, 1658 cm^{-1}, 2850 cm^{-1}, 2922 cm^{-1} and 3414 cm^{-1}. The similarities between (a) AgNP-Black seed and (b) Extract spectrums, few peaks indicate the presence of plant extract in the sample. The intense and wide peak that appeared at 3414 cm^{-1} denotes the presence of hydrogen-bonded N−H stretching vibrations of amide groups respectively (36). The peak at 2922 cm-1 may belong to the C−H stretching of the alkane group. The bands appearing in the range of 1700–1600 cm^{-1} and 1100–1000 cm^{-1} denote the C=O and C−O stretching vibrations, respectively. According to the previous study, the band appeared in the ranges of 1700–1600 cm^{-1} in the spectrum (a) indicates the formation of AgNP-Black seed capped with different bio moieties (37). The peak located at 1095 cm^{-1} could be assigned to the C−O stretching of vibration of carboxylic groups. The peak at 717 cm^{-1} is attributed to aromatic groups. These observations confirmed the presence of different biomolecules which might act as reducing and stabilizing agents during the synthesis of AgNP-Black seed (38).

FTIR results of AgNP-Clove indicate that absorption bands at 3415 (O–H stretching, H–bonded of alcohols, phenols, and N–H stretching of primary, secondary amines, amides of protein), 1600 (C=C stretching and N–H bend of alkenes and primary amines), 1384 (C-C stretching of aromatics) and 1016 (C-O stretching of alcohols, carboxylic acids, esters and ethers and C–N stretching of aliphatic amines). So, it is assumed that
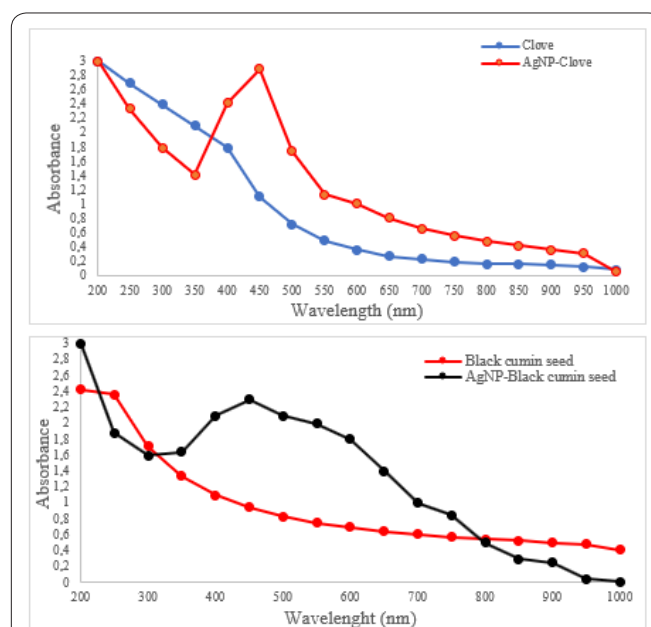
Figure 4. UV–visible spectra of AgNPs at different time intervals.
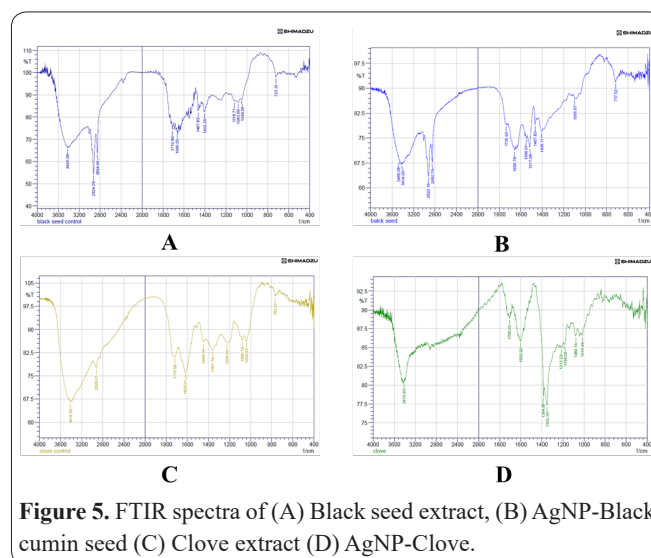
Figure 5. FTIR spectra of (A) Black seed extract, (B) AgNP-Black cumin seed (C) Clove extract (D) AgNP-Clove.

these biomolecules and some proteins are responsible for capping, stabilization, and reduction of Ag^+ to AgNPs. The FTIR analysis indicated the involvement of amides, alkanes, carboxyl, alcohols, and phenols group presented in the synthesized AgNP-Clove (20).

Antimicrobial activities of extracts and AgNPs

The antibacterial activity of extracts and AgNPs produced from this plant was evaluated against *P. mirabilis* using agar well diffusion and MICs. As shown in Tables (4), synthesized AgNPs are more effective against the negatively charged bacterial cell than the positively charged bacterial cell. Some works showed

Table 4. Inhibition zone diameter of extract and AgNPs against *P. mirabilis* in different concentrations.

Extracts and AgNPs	Inhibition zone diameter mm of *P. mirabilis* PM53				
	32 µg. mL^{-1}	64 µg. mL^{-1}	128 µg. mL^{-1}	256 µg. mL^{-1}	512 µg. mL^{-1}
Clove	13	10	17	5	20
C-AgNPs	25	27	22	25	35
Black cumin seed	3	2	3	7	5
B-AgNPs	13	10	19	17	23
Positive control (Gentamicin)			24		
Negative control (DMSO)			0		

that the formed AgNPs using plant extract were more toxic against positive pathogens than negative ones. By increasing AgNPs and plant extract concentration, the inhibition zone diameter also increased. In the case of plant extract, by decreasing in concentrations, no inhibitory was observed. It might be that the AgNPs had better penetration through the agar and consequently into cell bacteria than the plant extract due to the small size of nanoparticles.

The highest inhibition zone diameter was achieved for *P. mirabilis* (35 mm and 20 mm) for AgNP-Clove and clove extract at 512 µg. mL^{-1}. While the minimum inhibition zone diameter was recorded at 22 mm at 128 µg. mL^{-1} and 5 mm at 256 µg. mL^{-1} for AgNP-Clove and clove extract, respectively. However, the highest inhibition zone of both black seed and AgNP-Black cumin seed was recorded at 512 and 256 µg. mL^{-1} was 23 mm and 7 mm, respectively. And, the lowest inhibition zone was found at 64 µg. mL^{-1}. The MIC value was performed for *P. mirabilis*, demonstrating that the AgNPs have the maximum antibacterial efficacy to this microorganism (Table 5). The MIC of clove extract and C-AgNPs was 512 and 128 µg. mL^{-1} respectively. However, the value of MIC of both black cumin seed extract and B-AgNPs were 512 and 256 µg. mL^{-1} respectively.

Samuggam et al (39) performed the antimicrobial activity of silver nanoparticles (AgNPs) synthesis from S. mombin leaf extract with disc diffusion method. For the positive and negative control, ciprofloxacin commercial antibiotic disc and 10% DMSO were used, respectively. They found that the antimicrobial activity of ethanolic extract of *S. mombin* and AgNPs against *P. mirabilis*. The diameter of the inhibition zone of AgNPs is higher (21 mm) when compared with plant extract (9.33±0.33). Also, (40) were conducted the antibacterial activities of bio(AgNPs) toward P. mirabilis, this value reached 50 µg. mL^{-1}. For P. mirabilis, the AgNPs exhibited the lowest MBC at 100 µg. mL^{-1}. On the other hand, the well-diffusion method was assessed and was shown the highest antimicrobial activity against *P. mirabilis* (10 mm), when they were compared with both positive and negative control (25 and 2 mm, respectively).

The antimicrobial properties of silver nanoparticles are due to their penetration into the cell, binding to cell membrane receptors and membrane destruction, disruption of the process of intracellular energy production and release of cell sap (41). In fact, adhesion and destruction of the cell wall are one of the mechanisms of inhibition of gram-negative bacteria by silver nanoparticles (42). The production of free radicals by silver nanoparticles, which destroy cell membranes, is another antibacterial mechanism of these nanoparticles. Due to the interaction of silver ions with thiol groups, the interaction of silver nanoparticles and DNA prevents cell division and DNA replication, which ultimately leads to cell degradation (43).

Inhibition of protein and nucleic acid synthesis, as well as cell membrane degradation, is the common mechanism of nanoparticles and antibiotics to inhibit bacterial growth (44). In addition, there are several specific inhibitory mechanisms of silver nanoparticles: [1]: the attachment of nanoparticles to cell membranes and the creation of pores in them that disrupt membrane permeability and the release of intracellular contents (45); [2] the production of free radicals by silver nanoparticles that inactivate and destroy DNA molecules; [3]: Release of silver ions due to interaction between silver nanoparticles and thiol groups of bacterial proteins that inactivate many key bacterial proteins (46); [4]: Disruption of the ATP production process (47). Bacterial cells must undergo several gene mutations to counteract these effects, which is unlikely. On the other hand, *P. mirabilis*. genome carries antibiotic resistance loci towards different mechanisms of antimicrobial agents and metals, including swarming mobility, biofilm formation, enzymatic detoxification, and efflux systems by employing the PATRIC and PGAAP gene explanation services (48).

Inhibition of swarming activity of *P. mirabilis*

The swarming parameters expressed in terms of the number of concentric rings, diameters of swarm rings were determined to be reduced by different extracts and AgNPs concentrations. The pronounced reduction was observed in the colony diameter by extracts and AgNPs, in concentrations ranging from 32-512 mg. mL^{-1}. The negative control plate showed seven concentric rings. The number of rings was reduced to 1 in the medium, having 64 mg. mL^{-1} and 512 mg. mL^{-1} of clove extract and AgNPs-Clove, but in the black seed extract and AgNP-Black cumin seed, the ring numbers were reduced to 0 at 256 mg. mL^{-1} and 1 at 512 mg. mL^{-1}, respectively (Table 6).

Saleh et al. (49) reported different swarming behavior for isolates. The range of P. mirabilis isolates is between 21 and 42 mm. It has been observed that silver nanoparticles in sub-MIC concentrations prevent P. mirabilis from increasing in diameter. Our results are consistent with those reported by (50). The author showed that the production of a large number of virulence factors by *P. mirabilis*, such as hemolysin and protease, exacerbates infectious diseases. These virulence factors play an important role in increasing the motility of swarming cells and their movement from the urinary tract to other parts of the host tissue. Although not many studies have been done on the effect of silver nanoparticles on swarming cell formation; in some previous studies, the effect of nanoparticles on the rhl regulatory system that controls swarming motion has been mentioned (51). The results indicate the negative effect of silver nanoparticles on swarming behavior. It has also been shown that silver nanoparticles reduce swarming mobility by suppressing

Table 5. MIC, MBC, and tolerant level of extracts and AgNPs against *P. mirabilis* PM53 isolates.

Extracts and AgNPs	MIC (µg. mL^{-1})	MBC (µg. mL^{-1})	Tolerant level (MBC/MIC)	antibacterial efficacy
Clove (aqueous extract)	512	256	0.5	bactericidal
C-AgNPs	128	64	0.5	bactericidal
Black cumin seed (aqueous extract)	512	128	0.25	bactericidal
B-AgNPs	256	64	0.25	bactericidal

Table 6. Effect of different concentrations of *extracts* and AgNPs on swarming phenomenon of *P. mirabilis*.

Extracts and AgNPs	Concentration (µg. mL^{-1})	No. of concentric rings	Mean value of the diameter (± SD) of the last ring in mm	Mean value of the diameter (± SD) of 1st ring in mm
	32	5	22.67±2.05	6.33±3.09
	64	2	23.33±2.49	5.33±3.3
Clove	128	3	56.67±1.7	3.67±1.7
	256	3	21±0.82	5±2.16
	512	1	32±2.45	4.33±0.47
	32	4	62±1.63	9±0.82
	64	1	0±0.00	0±0.00
C-AgNPs	128	3	38±0.82	6±0.82
	256	2	9±0.82	3.33±2.62
	512	1	30±0.82	2.67±0.47
	32	4	31.57±1.25	5.33±2.87
	64	4	40.67±2.49	6.67±1.89
Black cumin seed	128	3	41±1.63	4.67±1.25
	256	2	40.76±0.94	5.67±0.47
	512	1	31.33±1.25	5±3.27
	32	4	31±2.36	4±2.16
	64	4	12±2.49	5.33±1.7
B-AgNPs	128	3	35.67±0.47	5.67±2.62
	256	0	39.67±3.3	7.33±1.7
	512	3	31.33±2.05	5±3.27
Negative control	0	7	62±0.251	9±1.21

fliL flagellar gene expression by up to 98% (52).

The swarming movement was the reason of combination sensory transduction and universal control operations. The swarming cells called for sensing and coupling of an assortment of cell-to-cell, environmental and intracellular signals, and involved adjusting the expression of gene networks key to physiological and morphological alterations. Alternations in gene *fla*A encoding flagellin protein and *flh*DC gene contributed to the upregulation of flagellin protein production, *C* and *wad* genes needed for the core region of LPS (53). Other genes implicated in flagellum construction drove the repression of Proteus rods' segregation and inhibition of swarming (49).

Biofilm formation assay

The biofilm mode of growth confers on the associated organisms a measurable decrease in antimicrobial susceptibility; for this reason, it is essential to know the times of growth and biofilm development. The ability of the strains to form biofilms on abiotic surfaces was evaluated by the crystal violet test. In this assay, all *P. mirabilis* isolates showed the ability to produce biofilms. Biofilm formation capability in these isolates was classified into three groups, strong biofilm producers (17.65%), moderate biofilm producers (39.22%), weak biofilm producers (27.45%), and non-biofilm former (15.69%) (Table 7). (6) were conducted an MTP assay of 176 isolates of *P. mirabilis* isolates, 162 (92.05%) were biofilm producers and 14 (7.95%) were non-producers. Of the biofilm producers (*n* = 162), 78 (48.15%) were moderate biofilm producers, whereas 62 (38.27%) and 22 (13.58%) were strong and weak biofilm producers, respectively. Similarly, (54) tested strains of *P. mirabilis* showed variable results in the aspect of biofilm

Table 7. Screening of *P. mirabilis* isolates for biofilm production by MPM assay.

Biofilm status	Biofilm formation of *P. mirabilis* isolates	
	No.	%
Strong biofilm former	9	17.65
Moderate biofilm former	20	39.22
Weak biofilm former	14	27.45
None biofilm former	8	15.69
Total	51	100

formation. Most clinical strains were put into the strong biofilm-former category (75, 20 and 5% were strong, moderate, and weak biofilm-formers, respectively). Two isolates from the strongest biofilm-forming P. mirabilis strains were selected for biofilm inhibition studies.

Immunological assessments of UTI patients

The serum from patients with UTI was tested for the presence of immunoglobulins (IgA, IgG, and IgM) and complement components (C3 and C4) by immunodiffusion plates. The result of IgG and IgA mean value (1311.13 ± 72.54 and 279 ± 21.31) respectively in the present study showed statistically significant difference among UTI patients in compared to controls groups (1089.88 ± 37.33 and 117.611 ± 4.19). On the other hand, serum levels of IgM among UTI patients were statistically non-significant increased with the mean values (153.331 ± 6.45) in compared to healthy controls (145.2±13.49) (Table 8 and Figure 6 A, B, C).

Complement components C3 was a statistically significant increase in UTI patients with the mean values (125.95±6.22 and 35.195±2.34) in compared to healthy controls with the mean values (55.191±9.64),

Table 8. Serum levels of Immunoglobulins' in UTI patients and control groups.

Immunoglobulin type	Patient	Control	*p*-value
IgG	1311.13 + 72.54	1089.88±37.33	0.0073
IgA	279+ 21.31	117.611±4.19	<0.0001
IgM	153.331±6.45	145.2 + 13.49	0.9981

Table 9. Serum complement component (C3 and C4) of UTI patients and control groups.

Immunoglobulin type	Patient	Control	p-value
C3	125.95 + 6.22	55.191±9.64	<0.0001
C4	35.195 + 2.34	34.371±1.22	0.9999

while serum level of C4 showed statically non-significant among UTI patients in comparison with the control group (and 35.195±2.34 and 34.371±1.22) respectively (Table 9 and Figure 7 A, B).

Discussion

Bacteria, commensals as well as pathogens, are constantly surrounding the human body, frequently as members of the microbiota. The early defense against bacterial infections depending on the various mechanisms of the innate and adaptive immune response, in which cytokines play a crucial role to initiate the inflammatory response (55,56). The innate and adaptive immune systems are responsible for preventing pathogenic bacteria from penetrating either by the protective barrier of the skin and mucous membranes or through the humoral and cellular immune response (57).

Immunoglobulins are a group of serum proteins with a crucial antimicrobial activity, IgM represents an indicator of recent infection, IgG levels increased in chronic infections, while IgA contains a secretory part that helps in reducing the mucosal and secretory based infections (58). The humoral immune response to antigenic or inflammatory challenges, such as infection either bacterial or other microorganisms, vaccination or trauma, has been proposed to comprise the polyclonal activation of memory B cells of unrelated specificity (59).

The results of this study showed a significant increase in the mean level of serum IgG and IgA (P ≤ 0.001) in UTI patients compared to the control group, while the level of IgM was elevated in UTI patients but showed no significant differences (p-value > 0.001). Serum antibodies found in UTI-positive patients have bactericidal activity (60). Antibodies in urine may resist UTI by preventing the adherence of bacteria to uroepithelial cells, the role of humoral immune response which increased IgG and IgA, IgM production were associated with UTI (61). Also, bacteria are killed by infected human serum through the lytic activity of the complement system. The results of the current study were in agreement with (61) and (62) who found that there were increases in the levels of immunoglobulins in UTI patients compared with the control group, also with the study of (63) and (64) who showed that *E. coli* was the major pathogen of UTI followed by *Proteus* spp, and they found that IgG and IgA concentrations significantly increased in UTI patients in comparison to control group while IgM concentration in the study of (63) was decreased in UTI patients. While it disagreed with the results of (65). This variation in results was might be due to the difference in
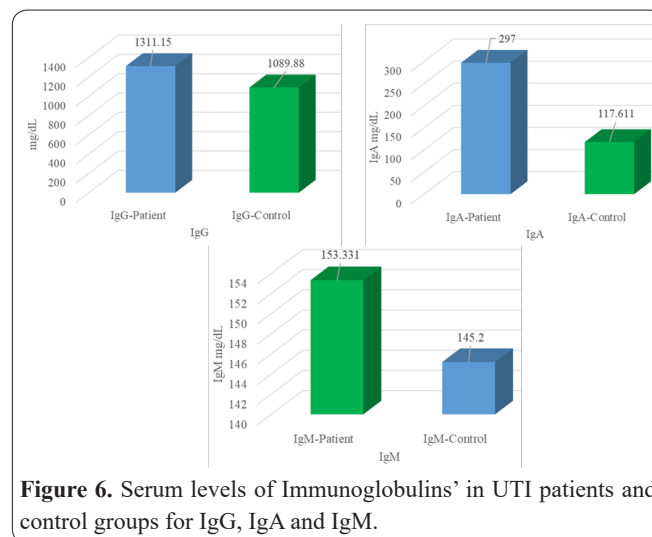
Figure 6. Serum levels of Immunoglobulins' in UTI patients and control groups for IgG, IgA and IgM.
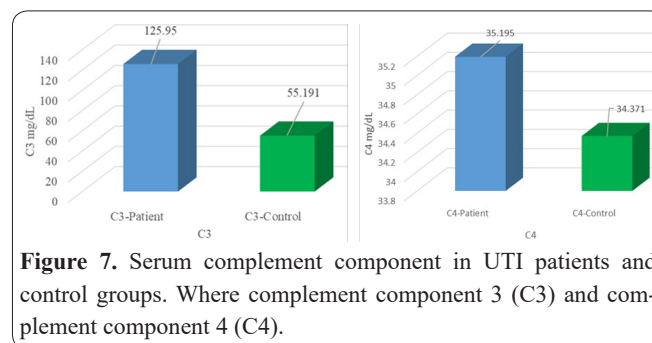
Figure 7. Serum complement component in UTI patients and control groups. Where complement component 3 (C3) and complement component 4 (C4).

study conditions and social status of study patients.

Elevation in serum concentration of IgG in patients suffering from UTI may be the reason for the significant increases in the concentration of complement components in patients suffering from UTI (64).

Increasing in serum mean levels of antibodies may be due to activation of B cell by antigenic stimulation that causes B cell to divide and differentiate into an antibody-producing cell called a plasma cell. Induction of production-specific antibody without the assist of T lymphocytes for example large molecular weight antigen with regular repeating epitopes involve Pneumococcal polysaccharide, flagellar and fimbrial antigen is IgM as a major antibody, this type of antigen called T cell-independent antigen (66). Some bacterial antigens can't induce B cells directly for producing immunoglobulins but by helping T lymphocytes called T cell-dependent antigen, the switch to other isotypes for example IgA and IgG, production needs the presence of cytokines and other signals secreted by locally responding T cells (58,66). Increased values of IgA in sera of UTI patients was due to immune reaction against causative agents of

infection, this result agreed with the findings of (61).

Urinary tract infection patients were showing more IgM values in sera than control individuals. Increased IgM values in patients groups were attributed to the surveillance of the immune system in the body and reaction against infection. The IgM undergoes first release within the primary immune reaction in acute inflammation to combat infection (66,67). This result agreed with the findings of (64,68). While it disagreed with the results of Azat, 2012 (65). This variation in results was might be due to the difference in study conditions and social status of study patients.

The hypergammaglobulinemia found in patients with UTI may reflect specific as well as non-specific polyclonal activation of B-lymphocytes. Many bacterial species are known to be capable of non-specific stimulation of B-lymphocytes and cause polyclonal B-cell activation, DNA-synthesis and proliferation and immunoglobulin synthesis (69). The quantitative estimation of total serum immunoglobulin in all classes may therefore help to make the differential diagnosis of whether a bacterial infection is chronic or acute.

Complement components C3 and C4 were increased in UTI patients in comparison to control groups. These results agreed with that reported by others (68) and disagree with the results of (70). Several studies have been conducted to assess the role of C3 in infectious diseases (70–73). The increasing of complement component C3 in the blood circulation of patients with UTI may return to the production of complement proteins by hepatocytes and several extrahepatic tissues that involved glomerular epithelial cells, endothelial cells, mesangial cells and human proximal tubular epithelial cells (74,75). The C3b fragment which produced by C3 split binds to fimbriae expressing on uropathogenic then C3b binds with Decay accelerating factor (CD55) has been located on the surface of human renal epithelial cells (74), CD46 can act as a human epithelial cell receptor for entering of opsonized uropathogenic *E coli* (76).

Infection, in general, caused an increase in the C3 component of the complement because this component is activated in classical and alternative pathways, while the elevation of the C4 component of the complement has occurred in the classical pathway more than an alternative pathway. UTI infection is a mixed infection, it causes by different types of bacteria some of them producing Exo-Toxins while others producing Endo-Toxins, so alternative pathways and classical pathways may be activated when the bacterial toxin is produced by bacteria while the classical pathway is activated by bacteria itself (68). Complement components have an important role in Inflammatory processes UTI infection attributed the increase of complement component production to the stimulation of the inflammatory mediators (77).

In addition, the C3 complement represents a critical component of the complement cascade, subserves several critical functions in human immune response and enhances bacterial killing and its levels correlate with infectious diseases (70). In addition, recurrent UTI is believed to be associated with the host immune system; Complement cascade activation is an effective immune mechanism that occurs in three different forms (the classic, alternative, and mannan-binding lectin) and is activated by pathogens. Regardless of the pathway, this activation causes the formation of C3 and C5 convertases, which in turn increases the production of bioactive compounds such as anaphylatoxins, opsonins, and membrane attack complex (70). Surrounding cells and recruited inflammatory cells then take the decisions about the quality and quantity of the mucosal response, leading to disease or protection. The epithelial cells are thus important players in the mucosal immune system; acting both as docking sites for the bacteria and as sensors of microbial attack. So far, several studies have been conducted on the effect of nanoparticles in biological fields (78-85). In this regard, it is better to investigate the relationship between the use of nanoparticles with some abnormalities and complications such as the effect on gene polymorphism (86), mitochondrial disorders (87), sexual disorders (88) and overall human health (89).

Conflict of interest

References

1.   Kantele AM, Palkola N V., Arvilommi HS, Kantele JM. Distinctive homing profile of pathogen-specific activated lymphocytes in human urinary tract infection. Clin Immunol 2008;128:427–34.

2.   Weichhart T, Costantino G, Poglitsch M, Rosner M, Zeyda M, Stuhlmeier KM, et al. The TSC-mTOR Signaling Pathway Regulates the Innate Inflammatory Response. Immunity 2008;29:565–77.

3.   Li K, Sacks SH, Sheerin NS. The classical complement pathway plays a critical role in the opsonisation of uropathogenic Escherichia coli. Mol Immunol 2008;45:954–62.

4.   Schappert SM, Rechtsteiner EA. Ambulatory medical care utilization estimates for 2006. Natl Health Stat Report 2008.

5.   Hamilton Miller JMT. Reduction of Bacteriuria and Pyuria Using Cranberry Juice. JAMA J Am Med Assoc 1994;272:588.

6.   Sun Y, Wen S, Zhao L, Xia Q, Pan Y, Liu H, et al. Association among biofilm formation, virulence gene expression, and antibiotic resistance in Proteus mirabilis isolates from diarrhetic animals in Northeast China. BMC Vet Res 2020;16:1–10.

7.   Armbruster CE, Hodges SA, Mobley HLT. Initiation of swarming motility by Proteus mirabilis occurs in response to specific cues present in urine and requires excess L-glutamine. J Bacteriol 2013;195:1305–19.

8.   Ibrahim HH, Aljeburi NR, Jebar MS, Gayeb MA, Mahdi SS, Kudder HA, et al. Effect of sub MIC for imipenem, amikacin and cefixime on growth and swarming of Proteus mirabilis. J Pure Appl Microbiol 2018;12:2241–4.

9.   Wang WB, Lai HC, Hsueh PR, Chiou RYY, Lin S Bin, Liaw SJ. Inhibition of swarming and virulence factor expression in Proteus mirabilis by resveratrol. J Med Microbiol 2006;55:1313–21.

10. Abbas HA. Antibacterial, anti-swarming and antibiofilm activities of local Egyptian clover honey against Proteus mirabilis isolated from diabetic foot infection. Asian J Pharm Res 2013;3:114–7.

11. Belas R, Suvanasuthi R. The ability of Proteus mirabilis to sense surfaces and regulate virulence gene expression involves fliL, a flagellar basal body protein. J Bacteriol 2005;187:6789–803.

12. Aritonang HF, Koleangan H, Wuntu AD. Synthesis of silver nanoparticles using aqueous extract of medicinal plants' (impatiens

balsamina and lantana camara) fresh leaves and analysis of antimicrobial activity. Int J Microbiol 2019;2019.

13. Javan bakht Dalir S, Djahaniani H, Nabati F, Hekmati M. Characterization and the evaluation of antimicrobial activities of silver nanoparticles biosynthesized from Carya illinoinensis leaf extract. Heliyon 2020;6:e03624.

14. Masum MI, Siddiqa MM, Ali KA, Zhang Y, Abdallah Y, Ibrahim E, et al. Biogenic synthesis of silver nanoparticles using phyllanthus emblicafruit extract and its inhibitory action against the pathogen acidovorax oryzaestrain RS-2 of rice bacterial brown stripe. Front Microbiol 2019;10:820.

15. He Y, Wei F, Ma Z, Zhang H, Yang Q, Yao B, et al. Green synthesis of silver nanoparticles using seed extract of: Alpinia katsumadai, and their antioxidant, cytotoxicity, and antibacterial activities. RSC Adv 2017;7:39842–51.

16. Ma Q, Fonseca A, Liu W, Fields AT, Pimsler ML, Spindola AF, et al. Proteus mirabilis interkingdom swarming signals attract blow flies. ISME J 2012;6:1356–66.

17. Zhang W, Niu Z, Yin K, Liu P, Chen L. Quick identification and quantification of Proteus mirabilis by polymerase chain reaction (PCR) assays. Ann Microbiol 2013;63:683–9.

18. Nikousaleh A, Prakash J. Antioxidant components and properties of dry heat treated clove in different extraction solvents. J Food Sci Technol 2016;53:1993–2000.

19. Yassin MT, Mostafa AA-F, Al-Askar AA. In vitro anticandidal potency of Syzygium aromaticum (clove) extracts against vaginal candidiasis. BMC Complement Med Ther 2020;20:1–9.

20. Lakhan MN, Chen R, Shar AH, Chand K, Shah AH, Ahmed M, et al. Eco-friendly green synthesis of clove buds extract functionalized silver nanoparticles and evaluation of antibacterial and antidiatom activity. J Microbiol Methods 2020;173:105934.

21. Kuppusamy P, Yusoff MM, Maniam GP, Govindan N. Biosynthesis of metallic nanoparticles using plant derivatives and their new avenues in pharmacological applications – An updated report. Saudi Pharm J 2016;24:473–84.

22. Sathishkumar M, Sneha K, Won SW, Cho CW, Kim S, Yun YS. Cinnamon zeylanicum bark extract and powder mediated green synthesis of nano-crystalline silver particles and its bactericidal activity. Colloids Surfaces B Biointerfaces 2009;73:332–8.

23. Elbeshehy EKF, Elazzazy AM, Aggelis G. Silver nanoparticles synthesis mediated by new isolates of Bacillus spp., nanoparticle characterization and their activity against Bean Yellow Mosaic Virus and human pathogens. Front Microbiol 2015;6:453.

24. Alavi M, Karimi N. Characterization, antibacterial, total antioxidant, scavenging, reducing power and ion chelating activities of green synthesized silver, copper and titanium dioxide nanoparticles using Artemisia haussknechtii leaf extract. Artif Cells, Nanomedicine Biotechnol 2018;46:2066–81.

25. Mondal AH, Yadav D, Mitra S, Mukhopadhyay K. Biosynthesis of silver nanoparticles using culture supernatant of shewanella sp. ARY1 and their antibacterial activity. Int J Nanomedicine 2020;15:8295–310.

26. Aygül A, Öztürk İ, Çilli FF, Ermertcan Ş. Quercetin inhibits swarming motility and activates biofilm production of Proteus mirabilis possibly by interacting with central regulators, metabolic status or active pump proteins. Phytomedicine 2019;57:65–71.

27. Hamasalih RM, Abdulrahman ZFA. Antibiofilm potency of ginger (Zingiber officinale) and quercetin against staphylococcus aureus isolated from urinary tract catheterized patients. Appl Ecol Environ Res 2020;18:219–36.

28. Pole SL. Single radial immunodiffusion (SRID). B. Gel immunodiffusion Tech. Res. Lab. Med., 1984, p. 143.

29. Al-Hakeim HK, Hussein HA. Serum cortisol, immunoglobulins and some complements among depressed patients. Indian J Clin Biochem 2008;23:76–80.

30. Ghasemzadeh A, Jaafar HZE, Rahmat A. Antioxidant activities, total phenolics and flavonoids content in two varieties of Malaysia young ginger (Zingiber officinale Roscoe). Molecules 2010;15:4324–33.

31. Chahardoli A, Karimi N, Fattahi A. Biosynthesis, characterization, antimicrobial and cytotoxic effects of silver nanoparticles using nigella arvensis seed extract. Iran J Pharm Res 2017;16:1169–77.

32. Shankar SS, Rai A, Ahmad A, Sastry M. Rapid synthesis of Au, Ag, and bimetallic Au core-Ag shell nanoparticles using Neem (Azadirachta indica) leaf broth. J Colloid Interface Sci 2004;275:496–502.

33. Rajeshkumar S. Synthesis of silver nanoparticles using fresh bark of Pongamia pinnata and characterization of its antibacterial activity against gram positive and gram negative pathogens. Resour Technol 2016;2:30–5.

34. Sharma S, Kumar S, Bulchandini BD, Taneja S, Banyal S. Green Synthesis of Silver Nanoparticles and Their Antimicrobial Activity against Gram Positive and Gram Negative Bacteria. Int J Biotechnol Bioeng Res 2013;4:341–6.

35. Pohlit AM, Rezende AR, Lopes Baldin EL, Lopes NP, De Andrade Neto VF. Plant extracts, isolated phytochemicals, and plant-derived agents which are lethal to arthropod vectors of human tropical diseases - A review. Planta Med 2011;77:618–30.

36. Suhas DP, Jeong HM, Aminabhavi TM, Raghu A V. Preparation and characterization of novel polyurethanes containing 4,4′-{oxy-1,4-diphenyl bis(nitromethylidine)}diphenol schiff base diol. Polym Eng Sci 2014;54:24–32.

37. Sathishkumar P, Preethi J, Vijayan R, Mohd Yusoff AR, Ameen F, Suresh S, et al. Anti-acne, anti-dandruff and anti-breast cancer efficacy of green synthesised silver nanoparticles using Coriandrum sativum leaf extract. J Photochem Photobiol B Biol 2016;163:69–76.

38. Harshiny M, Matheswaran M, Arthanareeswaran G, Kumaran S, Rajasree S. Enhancement of antibacterial properties of silver nanoparticles-ceftriaxone conjugate through Mukia maderaspatana leaf extract mediated synthesis. Ecotoxicol Environ Saf 2015;121:135–41.

39. Samuggam S, Chinni S V., Mutusamy P, Gopinath SCB, Anbu P, Venugopal V, et al. Green synthesis and characterization of silver nanoparticles using spondias mombin extract and their antimicrobial activity against biofilm-producing bacteria. Molecules 2021;26:2681.

40. Buszewski B, Railean-Plugaru V, Pomastowski P, Rafińska K, Szultka-Mlynska M, Golinska P, et al. Antimicrobial activity of bio-silver nanoparticles produced by a novel Streptacidiphilus durhamensis strain. J Microbiol Immunol Infect 2018;51:45–54.

41. Manivasagan P, Venkatesan J, Senthilkumar K, Sivakumar K, Kim SK. Biosynthesis, antimicrobial and cytotoxic effect of silver nanoparticles using a novel Nocardiopsis sp. MBRC-1. Biomed Res Int 2013;2013.

42. Sondi I, Salopek-Sondi B. Silver nanoparticles as antimicrobial agent: A case study on E. coli as a model for Gram-negative bacteria. J Colloid Interface Sci 2004;275:177–82.

43. Morones JR, Elechiguerra JL, Camacho A, Holt K, Kouri JB, Ramírez JT, et al. The bactericidal effect of silver nanoparticles. Nanotechnology 2005;16:2346–53.

44. Corrêa JM, Mori M, Sanches HL, Cruz AD Da, Poiate E, Poiate IAVP. Silver nanoparticles in dental biomaterials. Int J Biomater 2015;2015.

45. Raffi M, Hussain F, Bhatti TM, Akhter JI, Hameed A, Hasan MM. Antibacterial characterization of silver nanoparticles against E.coli ATCC-15224. J Mater Sci Technol 2008;24:192–6.

46. Patra JK, Baek KH. Antibacterial activity and synergistic anti-

bacterial potential of biosynthesized silver nanoparticles against foodborne pathogenic bacteria along with its anticandidal and antioxidant effects. Front Microbiol 2017;8:167.

47. Chen CY, Chen YH, Lu PL, Lin WR, Chen TC, Lin CY. Proteus mirabilis urinary tract infection and bacteremia: Risk factors, clinical presentation, and outcomes. J Microbiol Immunol Infect 2012;45:228–36.

48. McArthur AG, Wright GD. Bioinformatics of antimicrobial resistance in the age of molecular epidemiology. Curr Opin Microbiol 2015;27:45–50.

49. Saleh TH, Hashim ST, Malik SN, Laftaah Al-Rubaii BA. Down-regulation of fliL gene expression by Ag nanoparticles and TiO2 nanoparticles in pragmatic clinical isolates of Proteus mirabilis and Proteus vulgaris from urinary tract infection. Nano Biomed Eng 2019;11:321–32.

50. Senior BW. Investigation of the types and characteristics of the proteolytic enzymes formed by diverse strains of Proteus species. J Med Microbiol 1999;48:623–8.

51. Arunkumar M, Suhashini K, Mahesh N, Ravikuma R. Quorum quenching and antibacterial activity of silver nanoparticles synthesized from Sargassum polyphyllum. ||| Bangladesh J Pharmacol 2014;9:54–9.

52. Osonga FJ, Akgul A, Yazgan I, Akgul A, Ontman R, Kariuki VM, et al. Flavonoid-derived anisotropic silver nanoparticles inhibit growth and change the expression of virulence genes in Escherichia coli SM10†. RSC Adv 2018;8:4649–61.

53. Morgenstein RM, Szostek B, Rather PN. Regulation of gene expression during swarmer cell differentiation in Proteus mirabilis. FEMS Microbiol Rev 2010;34:753–63.

54. Ranjbar-Omid M, Arzanlou M, Amani M, Shokri Al-Hashem SK, Mozafari NA, Doghaheh HP. Allicin from garlic inhibits the biofilm formation and urease activity of Proteus mirabilis in vitro. FEMS Microbiol Lett 2015;362:fnv049.

55. Cruz F, Dambros M, Naber KG, Bauer HW, Cozma G. Recurrent Urinary Tract Infections: Uro-Vaxom®, a New Alternative. Eur Urol Suppl 2009;8:762–8.

56. Finer G, Landau D. Pathogenesis of urinary tract infections with normal female anatomy. Lancet Infect Dis 2004;4:631–5.

57. Claesen J, Spagnolo J, Ramos SF, Kurita K, Byrd A, Aksenov A, et al. Cutibacterium acnes antibiotic production shapes niche competition in the human skin microbiome. BioRxiv 2019:594010.

58. SOMPAYRAC LM. How the immune system works. John Wiley & Sons.; 2019.

59. Bernasconi NL, Traggiai E, Lanzavecchia A. Maintenance of serological memory by polyclonal activation of human memory B cells. Science (80-) 2002;298:2199–202.

60. Weichhart T, Haidinger M, Hörl WH, Säemann MD. Current concepts of molecular defence mechanisms operative during urinary tract infection. Eur J Clin Invest 2008;38:29–38.

61. Ethel S, Bhat GK, Hegde BM. Bacterial adherence and humoral immune response in women with symptomatic and asymptomatic urinary tract infection. Indian J Med Microbiol 2006;24:30–3.

62. Berwary NJA, Ahmed HA. Prevalence of Urinary Tract Infection and Its effect on the immunological parameters among Erbilian Women. Polytech J 2017.

63. Al-khafaf DMR. Study of some microbial and Immunological parameter in patients with Urinary Tract Infection in Al- Diwanyia city. Al-Qadisiyah Med J 2010;8:28–38.

64. Mahdi NB, Abbas SK, Ahmed KJ. Relationship among Some Immunoglobulins, Complement Protein C3 and Urinary Tract Infection of Women Caused by Gram Negative Bacilli in Kirkuk, Iraq. Int J Curr Res Acad Rev 2016;4:99–106.

65. Azat NFA. Evaluation of Serum (immunoglobulin G , M) in children with nephrotic syndrome relapse. J Fac Med Baghdad 2012;54:15–7.

66. PARIJA SC. Textbook of Microbiology & Immunology-E-book. Elsevier Health Sciences; 2014.

67. LEVINSON W, JAWETZ E. Medical microbiology and immunology: examination and board review, Appleton & Lange. 2010.

68. Essa RH, Al_Zubaidi HK, Rasool KH, Hussein NH. Study of some bacteriological and immunological parameters in urinary tract infection of pregnant women. Int Educ Res J 2016;2:8–14.

69. Dziarski R. Preferential induction of autoantibody secretion in polyclonal activation by peptidoglycan and lipopolysaccharide. II. In vivo studies. J Immunol 1982;128:1026–30.

70. Syukri M, Imran I, Harapan H, Sja'bani M, Astuti I, Soesatyo MH. Comparison of serum C3 complement levels between young women with recurrent urinary tract infection and healthy women. Alexandria J Med 2015;51:35–9.

71. Tsoni SV, Kerrigan AM, Marakalala MJ, Srinivasan N, Duffield M, Taylor PR, et al. Complement C3 plays an essential role in the control of opportunistic fungal infections. Infect Immun 2009;77:3679–85.

72. Kopf M, Abel B, Gallimore A, Carroll M, Bachmann MF. Complement component C3 promotes T-cell priming and lung migration to control acute influenza virus infection. Nat Med 2002;8:373–8.

73. Figueroa JE, Densen P. Infectious diseases associated with complement deficiencies. Clin Microbiol Rev 1991;4:359–95.

74. Selvarangan R, Goluszko P, Popov V, Singhal J, Pham T, Lublin DM, et al. Role of decay-accelerating factor domains and anchorage in internalization of Dr-fimbriated Escherichia coli. Infect Immun 2000;68:1391–9.

75. Sheerin NS, Zhou W, Adler S, Sacks SH. TNF-α regulation of C3 gene expression and protein biosynthesis in rat glomerular endothelial cells. Kidney Int 1997;51:703–10.

76. Li K, Feito MJ, Sacks SH, Sheerin NS. CD46 (Membrane Cofactor Protein) Acts as a Human Epithelial Cell Receptor for Internalization of Opsonized Uropathogenic Escherichia coli . J Immunol 2006;177:2543–51.

77. Botto M, Kirschfink M, Macor P, Pickering MC, Würzner R, Tedesco F. Complement in human diseases: Lessons from complement deficiencies. Mol Immunol 2009;46:2774–83.

78. Moradi S, Khaledian S, Abdoli M, Shahlaei M, Kahrizi D. Nano-biosensors in cellular and molecular biology. Cell Mol Biol 2018;64(5):85-90.

79. Darvishi E, Kahrizi D, Arkan E, Hosseinabadi S, Nematpour N. Preparation of bio-nano bandage from quince seed mucilage/ZnO nanoparticles and its application for the treatment of burn. J Mol Liq. 2021;339:116598.

80. Khaledian S, Noroozi-Aghideh A, Kahrizi D, Moradi S, Abdoli M, Ghasemalian AH, Heidari MF. Rapid detection of diazinon as an organophosphorus poison in real samples using fluorescence carbon dots. Inorg Chem Commun 2021;130:108676.

81. Darvishi E, Kahrizi D, Arkan E. Comparison of different properties of zinc oxide nanoparticles synthesized by the green (using Juglans regia L. leaf extract) and chemical methods. J Mol Liq 2019 Jul 15;286:110831.

82. Khaledian S, Kahrizi D, Balaky ST, Arkan E, Abdoli M, Martinez F. Electrospun nanofiber patch based on gum tragacanth/polyvinyl alcohol/molybdenum disulfide composite for tetracycline delivery and their inhibitory effect on Gram+ and Gram–bacteria. J Mol Liq 2021;334:115989.

83. Khaledian S, Kahrizi D, Moradi S, Martinez F. An experimental and computational study to evaluation of chitosan/gum tragacanth coated-natural lipid-based nanocarriers for sunitinib delivery. J Mol Liq 2021;334:116075.

84. Rahimi T, Kahrizi D, Feyzi M, Ahmadvandi HR, Mostafaei M. Catalytic performance of MgO/Fe2O3-SiO2 core-shell magnetic na-

nocatalyst for biodiesel production of Camelina sativa seed oil: Optimization by RSM-CCD method. Ind Crops Prod 2021;159:113065.

85. Olfati A, Kahrizi D, Balaky ST, Sharifi R, Tahir MB, Darvishi E. Green synthesis of nanoparticles using Calendula officinalis extract from silver sulfate and their antibacterial effects on *Pectobacterium caratovorum*. Inorg Chem Commun 2021;125:108439.

86. Ercisli M., Lechun, G, Azeez S, Hamasalih R, Song S, Aziziaram Z. Relevance of genetic polymorphisms of the human cytochrome P450 3A4 in rivaroxaban-treated patients. Cell Mol Biomed Rep 2021; 1(1): 33-41.

87. Aziziaram, Z., Bilal, I., Zhong, Y., Mahmod, A., Roshandel, M.

Protective effects of curcumin against naproxen-induced mitochondrial dysfunction in rat kidney tissue. Cell Mol Biomed Rep 2021; 1(1): 23-32.

88. Kazemi E, Zargooshi J, Kaboudi M, Heidari P, Kahrizi D, Mahaki B, Mohammadian Y, Khazaei H, Ahmed K. A genome-wide association study to identify candidate genes for erectile dysfunction. Brief Bioinforma 2021;22(4):bbaa338. https://doi.org/10.1093/bib/bbaa338

89. Mojadadi A, Au A, Salah W, Witting P, Ahmad G. Role for selenium in metabolic homeostasis and human reproduction. Nutrients 2021;13(9):3256.